Effects of Plasticizers on the Rheological Behavior of Ethylene-Vinyl Acetate (EVA) Copolymer Using an Online Capillary Rheometer

Praneeth D. Bangaru[1,*], Terezie Pospíšilíková[2], Tharcisse Renzahoduke[1] and Jens Schuster[1]

[1]*Hochschule Kaiserslautern, Pirmasens, Germany*

[2]*Univerzita Tomáše Bati ve Zlíně, Zlín, Czech Republic*

Abstract: The objective of this work is to find an appropriate ethylene vinyl acetate (EVA) copolymer-plasticizer blend for potential use in further extrusion-based additive manufacturing (AM) processes, such as FGF technology applications. Plasticizers, as additives, soften the materials and improve material flow in polymer processing systems. In the current work, plasticizers used were paraffin oil (PO), triethyl citrate (TEC), and di(propylene glycol) dibenzoate (DPGDB). The plasticizer concentrations used in the blends were 1, 3, 5 and 7 phr (parts per hundred resin). Increasing plasticizer content resulted in an increase in the melt flow rate (MFR) compared to the non-plasticized EVA; however, the rate of increase was strongly influenced by the type of plasticizer used. DSC results showed a reduction in melt temperature and an increase in degree of crystallinity. Viscosity measurements for blends with 5 and 7 phr were made using an online capillary rheometer. Bagley and Rabinowitsch corrections were applied to obtain the true shear viscosity. A noticeable drop in the viscosity with increasing shear rate in both plasticized and non-plasticized EVA has been detected; however, variation in viscosity was observed with changes in processing temperatures regardless of the plasticizer type and content within the measured shear-rate range.

Keywords: Ethylene vinyl acetate, Plasticizer, EVA melt viscosity modification, Bagley correction, Rabinowitsch correction.

1. INTRODUCTION

EVA is a random linear copolymer of low-density polyethylene (LDPE) and vinyl acetate (VA); it consists of amorphous-flexible, polar units of VA and rigid crystalline, non-polar polyethylene segments [1-3]. Polymerizing VA with ethylene can disorder the crystal regions of PE and will eventually lead to a low-crystalline material. The varying amounts of VA in the copolymer are responsible for the properties of the material; increasing VA content lowers the crystallinity [2-5]. At some point, at VA content up to 50%, the material becomes completely amorphous. Additionally, VA is more polar in nature than ethylene, which increases the polarity of the material, which leads to much more versatility of EVA applications across different industries [2, 5, 6]. Polymer melts during the flow exhibit complex rheological behavior of elasticity, shear thinning and yield stress; the underlying reason is that due to microstructural changes and long entangled polymer chains, which continuously change their orientation and degree of entanglement under and in the direction of flow [7, 8]. In EVA copolymer, the degree of branching lowers with the increase in the VA content due to the inhibition of cyclic intermediates by the VA that are involved in the occurrence of short branches [1]. Higher molecular weight (MW) increases the viscosity due to more entanglement of long polymer chains, which restricts the melt flow. Thus, a higher MW results in a higher viscosity [1, 3].

EVA is widely processed using melt extrusion methods. The optimal processing temperature for pure EVA is ~155°C, where it does not undergo degradation at higher shear rates for extended periods [3, 9]. In general, high processing temperatures lower the viscosity. However, the decrement is subject to processing time and temperatures. At extrusion temperatures above 160°C, the time-dependent viscosity exhibited a V-shaped variation (decreasing viscosity → increasing viscosity); the minimum viscosity of ~10 Pa·s was reached after 25 min of processing time for 18 wt% of VA. The subsequent increase in viscosity is likely due to MW growth and onset of crosslinking during prolonged thermal processing [3, 9]. A similar trend with free volume size (in nm) is observed in the literature. Higher VA content leads to an earlier transition and accelerated degradation under similar processing conditions. In general, semi-crystalline polymers possess a higher thermal conductivity in comparison to amorphous polymers due to the closed packing of polymer chains in the crystalline regions; however, due to the presence of VA, EVA has lower thermal conductivity in comparison to most of the thermoplastics, having a value of 0.311–0.34 W/(m.K) [5]. The low thermal conductivity of the polymer may lead to higher thermal gradients in the axial and radial directions at higher 3D-printing speeds

*Address correspondence to this author at the Hochschule Kaiserslautern, Pirmasens, Germany;
E-mail: praneeth.bangaru@hs-kl.de

Received on 12-09-2026 Accepted on 22-10-2026 Published on 05-11-2026

E-ISSN: 2410-4701/26

[10]. These gradients may prevent the melt from reaching isothermal conditions, potentially affecting the material flow due to local increase in viscosity.

Granular-based (FGF) 3D printers effectively have the advantage of eliminating the need for filament manufacturing, which significantly enlarges the choice of 3D-printable material. Small-format pellet 3D printers use lower screws. L:D ratios: the smaller the screw diameter, the shorter the screw, leading to lightweight print heads for high-speed 3D printing [11, 12]. A lower L:D ratio has a comparatively shorter residence time for melting and homogenization. Increasing the temperature slightly would facilitate proper melt transport and continuous melt of extrudates by lowering the melt viscosity [11]. However, with an increase in the temperature and screw speed (extrusion multiplier), the extrusion rate increment would be non-linear [11]. In temperature-restricted or tightly controlled processing, beyond a certain limit, varying temperature is not an appropriate choice, *e.g*., in foam 3D printing. At the selected temperature, if the material has a higher melt viscosity, an inappropriate material flow rate and material dosing is attained; consequently, the stepper motor would struggle to rotate the screw continuously due to extreme resistance caused by the high viscosity [11, 13]. High melt viscosity is also a limiting factor in FGF 3D printing, where the required steps/mm increase with increasing melt viscosity [13]. Therefore, altering the melt viscosity through plasticization would also be a viable method; the required flow behavior can be attained without increasing the temperature and screw speed. In general, for foaming expansions, the morphology of the foam cells—size and density—is related to the viscosity of the polymer matrix, suggesting the need for viscosity alteration for the enhanced foaming [4].

Previous studies have verified that the shear rate and MW have significant influence on the rheological responses [1, 5]. Zimmermann *et al*. [4] reported that, due to negative T_g and inherent elastomeric properties, EVA is not commonly plasticized, and furthermore, it has poor compatibility with most of the conventional plasticizers [8]. However, only a few studies [5, 14] have published on the plasticization of EVA. Plasticizers are the most common additives: low-MW and low-viscosity compounds that directly interact with the polymer chains at the molecular level, which lower cohesive forces between polymer chains and improve flexibility, molecular mobility and viscoelastic response when added to polymeric materials [8, 14]. Other than making the material more flexible by decreasing the T_g, the addition of plasticizer could be beneficial in many other ways: increased compatibility between additives and polymer in blends, improvement of the optical clarity and increase in gas permeability for the production of polymeric foams [8]. The compatibility of a plasticizer with a polymer depends on solubility parameters, polarity, and hydrogen-bonding characteristics similar to that of the polymer. If these parameters are met, it is assumed that the selected plasticizer should be compatible with the selected polymer [8]. Polarity is an important parameter for the proper polymer-plasticizer interaction. Polar polymers blend readily with the polar plasticizers, and they do not mix with the nonpolar plasticizers. The selected plasticizer should have a suitable affinity towards the polymer matrix; as a result, plasticizer molecules enter in between the permolecular branches in polymers, resulting in increased free volumes and chain mobility [14].

Among the commonly used plasticizers, citrate-based plasticizers are popular and highly recommended for VA-based copolymers [8]. Hydrocarbon oils are widely used as processing aids. PO's are classified under hydrocarbon oils and consist of linear and branched alkanes with low polarity; those with high purity are considered the most stable compounds [8, 15]. PO is thermally stable until 200°C. However, in higher concentrations, it poses a risk of bleeding out from the material [15]. Di-benzoates are compounds with two aromatic benzene rings and ester groups; benzoate-based plasticizers are highly recommended for EVA copolymers [8]. Dipropylene glycol dibenzoate (DPGDB) is a polar plasticizer due to the presence of polar ester groups. The presence of a plasticizer facilitates better chain mobility by providing more degree of freedom, thereby reducing the energy required during processing and increase overall efficiency. However, the plasticizer concentration should be carefully adjusted for 3D printing applications, while considering initial and interlayer consolidation. A higher plasticizer content would typically affect these processes.

The objective of this study was to reduce the melt viscosity of EVA by using suitable plasticizers: TEC, PO and DPGDB and to identify a suitable EVA-plasticizer blend for potential application in FGF 3D printers with low *L/D* ratio screws, where the inherently high melt viscosity of EVA results in high melt resistance and affects continuous screw operation. The main objective is to study the viscosity of the blends over a wide range of shear rates to understand their rheological behavior under processing conditions. In an attempt to lower the melt viscosity and improve the suitability for low-temperature 3D printing, EVA containing 27.5 wt.% VA with different plasticizer loadings was studied and the effects were evaluated using thermal and rheological methods.

2. METHODS AND MATERIALS

2.1. Materials

Commercial-grade EVA (ExxonMobil™ EVA 7028) was procured from TER Chemicals GmbH & Co. KG (Hamburg, Germany). The material grade had a density of 0.951 g/cm³, a VA content of 27.5 wt.%, a melt flow index of 7 g/10 min, and a melting point of 75°C. Three plasticizers were used in the current work: paraffin oil, triethyl citrate (density: 1.14 g/cm³; Carl Roth GmbH + Co. KG, Karlsruhe, Germany) and di(propylene glycol) dibenzoate (purity ≥75% from Merck Sigma-Aldrich, Darmstadt, Germany). All plasticizers were used as received.

2.2. Compounding of EVA/Plasticizer Blend

To ensure low moisture content, EVA pellets were pre-dried in an oven for 48 h at 35°C before processing. Pre-experiments were conducted to analyze the concentration of plasticizer; based on that, compositions were prepared by varying the plasticizer concentration at 1, 3, 5 and 7 phr, whereas EVA was maintained at 100 parts by weight for every composition. EVA pellets and plasticizer were compounded using a laboratory-scale twin-screw extruder fitted with a slit die. The screw speed was maintained at 25-30 RPM and the barrel temperatures were at 45°C, 60°C, 80°C, and 100°C (hopper to die).

Subsequently, the extrudates were further granulated and re-extruded in filament form using a capillary die with similar process parameters as mentioned above to ensure the homogeneous mixing of the EVA/plasticizer blend. The filaments were then pelletized into short cylindrical pellets and used for subsequent experiments. Pure EVA (100 phr) was used as reference material. Three plasticizers, TEC, PO and DPGDB, were mixed with EVA at 1, 3, 5 and 7 phr, resulting in twelve blends coded as 1_TEC, 3_TEC, 5_TEC, 7_TEC; 1_PO, 3_PO, 5_PO, 7_PO; and 1_DPGDB, 3_DPGDB, 5_DPGDB and 7_DPGDB. Compositions measured at 100 and 150°C were identified by adding the temperature to the end of the sample code. For example, 5_PO_150 represents the 5_phr PO blend tested at 150°C, while EVA_100 represents pure EVA tested at 100°C.

Rheological Investigation

MFI (index of fluidity) is most widely used in industrial polymer processing due to its ease, simplicity and rapid measurement [16]. In principle, it can also be used to assess the basic rheological characteristics; however, the important drawback is that MFI measures flow behavior at a single, low shear rate, which lies in the Newtonian plateau of the viscosity curve, so it may not accurately predict how these materials will perform during industrial processing conditions where flow is described by the polymer's dynamic viscosity, which, in turn, is dependent on shear rate [13, 16, 17]. Additionally, there is no possibility of applying the Bagley correction to the measured data [17]. The most important limitation is that MFI data do not accurately represent the flow conditions of extrusion and injection molding. These processes require, by and large, higher shear rates. These drawbacks paved the way for different testing methods such as online viscosity and capillary rheometers. The capillary viscometer has been most commonly used for measuring viscosity; nevertheless, this offline measurement has the drawback of change in the rheological behavior and a significant time lag between production and detection of quality problems [7, 16]. Many authors have addressed the in-process (online) viscosity measurements directly using extruders [7, 16, 18]. Capillary and slit geometry dies have been employed at the end of the extruder. Material is fed through the die, where shear stress (τ) is associated with the pressure drop, measured by the pressure transducer (P_t) at the die entrance [7, 18]. Rod capillary dies are commonly used for online viscosity measurements in single-screw extruders. Moreover, this method of measuring viscosity is particularly suitable because the measurement method is similar to that of the FGF process, where dynamic viscosity data are directly relevant to understanding the material flow behavior in FGF processing [13]. Capillary dies are often described by the length-to-diameter (*L/D*) ratio. Capillary rheology data are subjected to corrections for the die entry pressure loss and for the deviation between apparent and true wall shear rate caused by non-Newtonian behavior. The Bagley and Weissenberg-Rabinowitsch corrections are applied to obtain the true wall shear stress (τ_w) and true wall shear rate (γ_w), respectively [17]. A corrected true viscosity (η_w) is derived from apparent shear viscosity (η_a) in Pa·s using Equation (1). The set of equations below is presented to obtain the true viscosity in a step-by-step manner [7, 13, 16-19].

$$\eta_a = \frac{\tau_a}{\dot{\gamma}_a} \tag{1}$$

Apparent shear stress (τ_a) in Pa is a measure of shear stress at the capillary wall (cylindrical channel) and is calculated as follows:

$$\tau_a = \frac{\Delta P}{L} \cdot \frac{R}{2} \tag{2}$$

Apparent wall shear rate ($\dot{\gamma}_a$) in (1/s) is

$$\dot{\gamma}_a = \frac{4}{\pi} \cdot \frac{\dot{Q}}{R^3} \tag{3}$$

Where ΔP is the pressure loss as the polymer flows through the capillary, L is the capillary length (mm), R is

the capillary radius (mm) and $\dot{Q}$ is the volumetric flow rate.

When a polymer melt flows through the capillary die channel, pressure loss is caused not only by friction inside the capillary but also by pressure loss at the capillary entrance due to the contraction/funneling of the flow from a larger to a smaller diameter, which leads to incorrect viscosities if not corrected. ΔP_F is the pressure drop over the fully developed flow region, which extends along the length of the capillary F_L; refer to Figure **1**.

$$\Delta P_{measured} = \Delta P_{inlet} + \Delta P_F + \Delta P_{outlet} \quad (4)\ [17]$$

Therefore, to obtain a τ_w, the pressure drop is measured using different dies with decreasing lengths (different *L/D* ratios), and a linear extrapolation is plotted until *L/D* = 0.

$$\Delta P_c = \Delta P_{measured} - \Delta P_b \quad (5)$$

Extrapolated value ΔP_b represents the Bagley correction, which accounts exclusively for the pressure losses at the capillary inlet and outlet [19]. After applying the Bagley correction with *L/D* = 40, the true shear stress τ_w (Pa) capillary die is given as follows:

$$\tau_w = \frac{\Delta P_c\, R}{2\, L} \quad (6)$$

Where ΔP_c is the corrected pressure value calculated using Equation (5). Newtonian flow behavior is assumed when calculating $\dot{\gamma}_a$ (parabolic velocity profile and negligible wall slip), but in practice, due to shear-thinning behavior in polymer melts (flow exponent n < 1), there is non-uniform flow with higher wall shear rates [19-21]. The Rabinowitsch correction assumes non-Newtonian pseudoplastic behavior of the material; therefore, $\dot{\gamma}_w > \dot{\gamma}_a$, where $\dot{\gamma}_w$ (1/s) is the true shear rate. This causing the viscosity curve to shift downward in standard shear rate vs. viscosity plots [17]. According to Rabinowitsch, the correction of apparent shear rate and determining $\dot{\gamma}_w$ in rod capillaries is given as

$$\dot{\gamma}_w = \frac{\dot{\gamma}_a}{4}(3 + s) \quad (7)$$

Where s is the slope of the log-log plot between apparent shear rate ($\dot{\gamma}_a$) and true wall shear stress (τ_w).

$$s = \frac{dlog(\dot{\gamma}_a)}{dlog(\tau_w)} \quad (8)$$

Similarly, true viscosity η_w in Pa·s after corrections can be calculated using Equation (9), which relates corrected wall shear stress to the corrected wall shear rate.

$$\eta_w = \frac{\tau_w}{\dot{\gamma}_w} \quad (9)$$

The shear-rate dependence of polymer viscosity was described by the Carreau-Yasuda (CY) model as described in Equation (10), which consists of five parameters and has an advantage over the power-law model [20]. The CY model fits both low and high shear rate conditions well, which covers a wide range of polymer processing conditions [5]. Interpolation can be performed easily by adjusting the parameters, and additionally, extrapolation can also be made with greater confidence. Obtained viscosity data from *L/D*=40 were fitted using the CY model to obtain the shear rate-dependent viscosity plot covering the range from low to high shear rates to quantify the shear-thinning behavior of the polymer melt [21].

$$\eta = \eta_0[1 + (\lambda\dot{\gamma})^a]^{\frac{n-1}{a}} \quad (10)$$

η_o is the zero-shear viscosity (Pa·s) in the Newtonian regime, while λ, n and a are fitted parameters. Where λ represents the relaxation time (s) marking the transition between linear and nonlinear

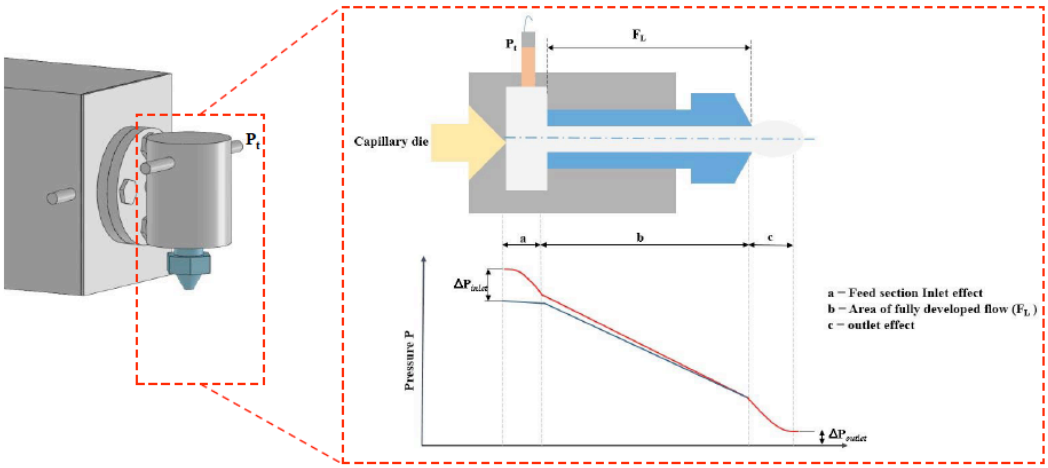


Figure 1: Inlet and outlet pressures in the rod capillary die.

behavior, *n* is the power-law index determining the shear-thinning property, and *a* is the Yasuda transition control factor of the viscosity function, as shown in Figure **2** [20]. During parameter fitting, a was fixed at 2 for all compositions to ensure stable regression with the experimental data.

Initial preliminary testings were conducted using a commercially purchased FGF 3D printer equipped with a screw with an L/D ratio of 7.8, a barrel diameter of 35 mm and a length of 80 mm. Print parameters were developed at different processing temperatures for pure EVA, resulting in shear rates (calculated from Equation (3)) ranging from 70 to 180 s^{-1} using a 0.8 mm nozzle.

In the current work, a HAAKE Rheomix 252 single-screw extruder (SSE) was used for viscosity measurements. It consists of a screw with an *L/D* ratio of 25:1 and a maximum speed of 200 rpm. The pressure transducer P_t (at the die) is rated for a maximum pressure capacity of 700 bar. The extruder barrel is divided into 4 sections: feed, transition, mixing and die. During rheology experiments for all the compositions, constant temperatures were maintained throughout the experiments for feed zones and transition and mixing zones (45°C, 60°C and 80°C). However, two different temperatures were used for selected compositions in the zone near the capillary die (100°C and 150°C) to assess the viscosity at low temperature and standard EVA processing temperatures, as mentioned by Zhang *et al*. [3].

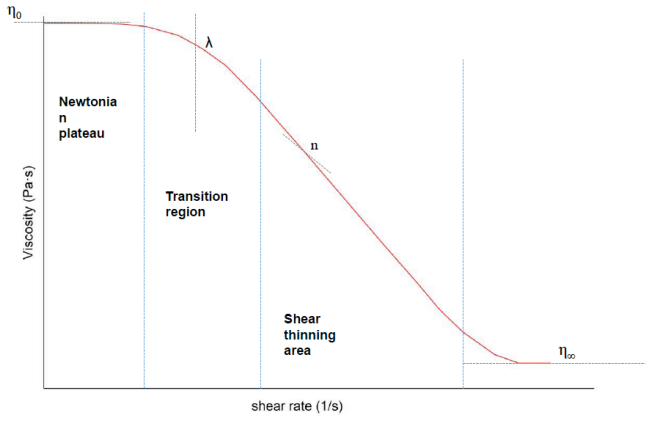


Figure 2: Principle viscosity of CY model.

The extruder consists of a die head, to which capillary dies can be fitted and exchanged. Rod capillary dies of the same diameter (1 mm) and different lengths (10D, 20D and 40D) were used for Bagley correction, as shown in Figure **3**. Measurements were performed in the order from the longest to the shortest die, *i.e*., 40D, 20D and 10D. Bagley and Rabinowitsch-Weissenberg corrections and CY model regression parameters were obtained from PolySoft OS software (Thermo Fisher). Regression analysis and plotting were performed using OriginPro software.



Figure 3: Rod capillary dies with different L/D ratios.

2.3. Melt Flow Index

MFR measurements were conducted using a Göttfert MP-D melt flow indexer (Germany) with a capillary die of *L/D* = 8:2.095 mm. All the compositions were tested according to ASTM D1238, using a test load of 2.16 kg and at a test temperature of 190°C, with a pre-heating time of 4 min. The material was allowed to extrude through the MFI capillary die for 10 min, and extrudates were collected and weighed using a high-precision weighing scale. The values reported are the average of three independent replicates. MFR experimental data were used as an initial screening method to identify the influence of plasticizers. Based on these results, the best of the compositions were selected, and viscosity measurements were carried out for subsequent rheological analysis.

2.4. Differential Scanning Calorimetry

Thermal properties of plasticized EVA were measured by differential scanning calorimetry (DSC). DSC measurements were carried out with a Phoenix F1 204 from NETZSCH (Selb, Germany) with the nitrogen flow (20 mL/min) and a heating/cooling rate of 10°C/min from −50°C to 150°C. The crucible types used were concavus aluminum, with pierced lids. The effect of plasticizer on melting temperature (T_m) and degree of crystallinity (X_c) was analyzed using the 2nd heating cycle.

$$X_c(\%) = \frac{\Delta H_{m2}}{\Delta H_{m0}(1-\emptyset)} \times 100 \quad (11)$$

X_c in % is determined according to Equation (11) [5]. Where ΔH_{m2} is the melting enthalpy of the second heating curve, ΔH_{mo} represents the theoretical enthalpy of melting for 100% crystalline polyethylene, which is assumed to be 293 $J \cdot g^{-1}$, and $\emptyset$ represents the weight fraction of plasticizer in the blend [4, 5, 22].

3. RESULT AND DISCUSSIONS

3.1. MFR

The images below and Table **1** show the effect of plasticizer on the MFI of EVA. Each figure depicts the varying plasticizer content along with pure EVA (denoted as EVA). Pure EVA showed a slightly lower value of 5.97 compared with the manufacturer's reported value, which can be ascribed to the different experimental conditions and thermal history of the material. Anticipated trend observed among all the types was that as the plasticizer content increases, the MFI value tends to increase, but the rate of increase differed among the blends.

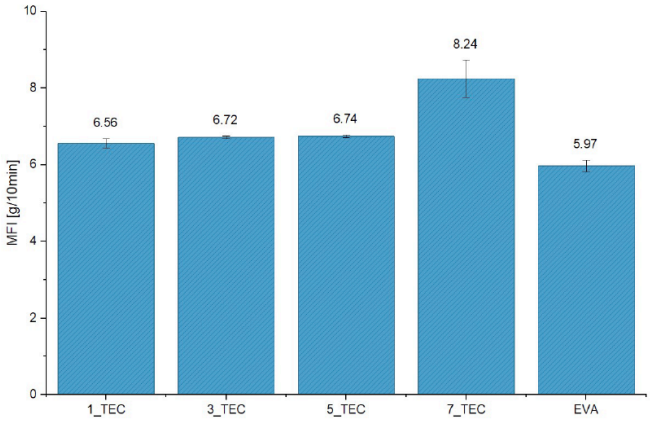


Figure 4: Variation of MFI-EVA/TEC.

For instance, in the case of TEC (as seen in Figure **4**), from 1 to 7 phr, the MFI increased from 6.56 to 8.24 g/10 min. It is important to note that at 1, 3 and 5 phr, a negligible difference was observed and at 7 phr, a sudden increase from 6.7 to 8.2 g/10 min can be seen.

During the melt compounding of 7_TEC composition, plasticizer bleed-out was observed at the die exit, where droplets of TEC appeared along with the extruded material, suggesting limited compatibility at higher plasticizer loadings. Moreover, limited miscibility at higher plasticizer concentrations is very likely due to polarity mismatch between the plasticizer and ethylene segments of EVA, which resulted in poor mixing and subsequent bleed-out during processing. Consequently, the MFI value of 7_TEC should not be

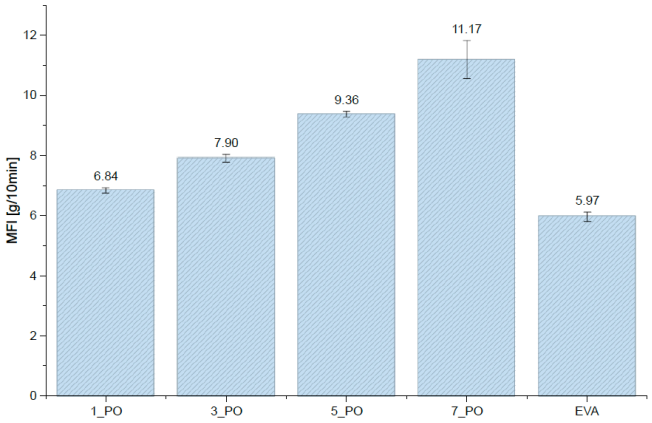


Figure 5: Variation of MFI-EVA/PO.

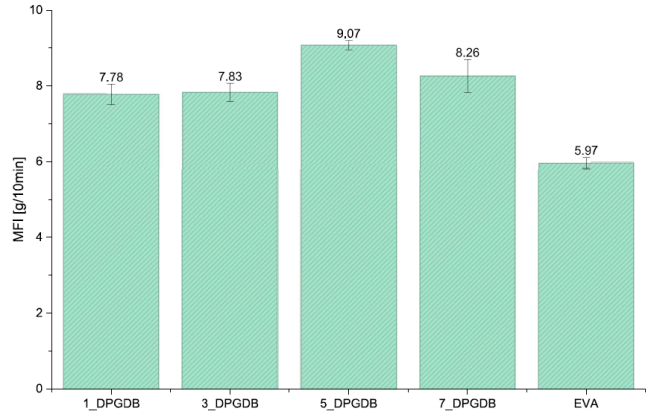


Figure 6: Variation of MFI-EVA/DPGDB.

interpreted as the true value of the blend. A linear increase in MFI was observed in EVA/PO from 6.84 to 11.17 g/10 min, as illustrated in Figure **5**. Paraffin oil, an industrial mineral oil, is considered a low-polarity plasticizer [14]. Being a low-polarity plasticizer, PO showed good plasticizer-matrix interaction, especially with the non-polar ethylene segments of the EVA, promoting chain flexibility. Consequently, the 7_PO blend exhibited the highest MFI value among all the blends. It is important to mention that the MFI is a low-shear process, where most of the EVA/PO blends remain in the Newtonian plateau, as reported by Standring *et al*. [5], although varying the paraffin wax content lowered the flow resistance at low shear rates. DPGDB is a highly polar plasticizer compared with the PO and TEC. At lower concentrations, this plasticizer

Table 1: Melt Flow Index Values in g/10 min

Composition	phr			
	1	3	5	7
EVA/TEC	6.56±0.12	6.72±0.03	6.74±0.04	8.24±0.49
EVA/PO	6.84±0.08	7.90±0.13	9.36±0.09	11.17±0.63
EVA/DPGDB	7.78±0.27	7.83±0.24	9.07±0.13	8.26±0.43
EVA	5.97±0.15			

has enhanced the flow, as seen in Figure **6**, suggesting a strong interaction of DPGDB with the polar VA segments. At the plasticizer concentration of 7 phr, the MFR was slightly reduced to 8.26 g/10 min. To rule out the possibility of an experimental error, the composition was re-compounded and re-tested. Nevertheless, similar results were obtained, indicating the saturation point or poor compatibility of DPGDB with the EVA matrix at concentrations of 7 phr.

3.2. DSC

DSC thermograms of the TEC, PO and DPGDB blends, along with pure EVA, are presented in Figure **7**. T_g could not be evaluated from the DSC cycle due to very small changes in heat capacity and the overlapping melting effect, making it difficult to do a reliable comparison between the blends. The second DSC heating run resulted in a broad melting endothermic peak for all the blends. The VA groups disrupt the polyethylene crystallites, which results in a wide distribution of crystallite sizes in the EVA matrix, which leads to the broad endothermic peak [22]. All the plasticized blends exhibit a slight reduction in T_m of ~0.3-2.0 °C in comparison to the non-plasticized EVA; the highest variation was seen in the 5 and 7 phr PO blends, where T_m was 72.7°C and 72.1°C.

This reduction is due to the softening effect of plasticizers and inducing weaker intermolecular interactions [15]. Additionally, the degree of crystallinity of the plasticized composition varied between 28.80% and 33.29% relative to pure EVA, which showed a degree of crystallinity of 28.20%. However, no significant correlation was observed between degree of crystallinity and increasing plasticizer content. The EVA/PO blend showed a higher degree of crystallinity at lower PO contents, followed by a gradual decrease to a value of 28.80% at a PO content of 7 phr. The DSC parameters are presented in Table **2** within each table cell; the values of melting temperature (T_m) and degree of crystallinity (X_c) are separated by a semicolon.

3.3. Online Rheology using SSE

For the online capillary rheological analysis, only the 5 and 7 phr plasticized compositions at 100 and 150°C were considered and compared with non-

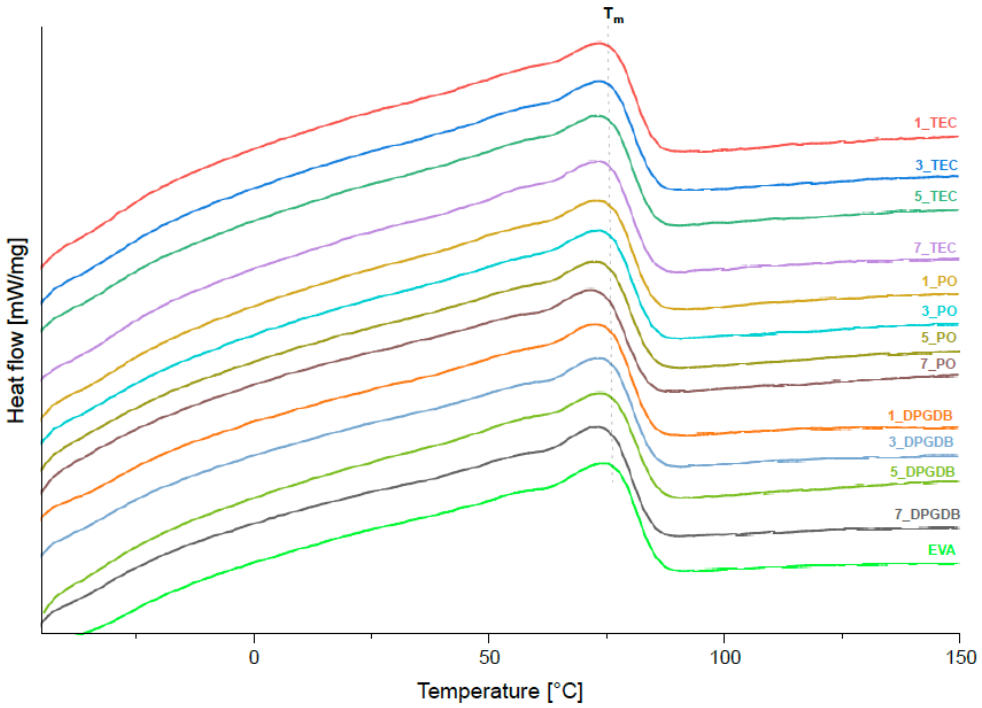


Figure 7: DSC scans of the plasticized blends and EVA material.

Table 2: Melting Temperature (T_m) and Degree of Crystallinity (X_c) of Neat EVA and Plasticized EVA Blends

Composition	phr			
	1	3	5	7
EVA/TEC	73.5 ; 32.0	73.2 ; 32.0	72.9 ; 32.12	73.1 ; 33.29
EVA/PO	73.4 ; 31.15	73 ; 30.28	72.7 ; 29.93	72.1 ; 28.80
EVA/DPGDB	73.4 ; 29.65	73.4 ; 29.87	73.2 ; 31.46	73.2 ; 31.27
EVA	74.2 ; 28.2			

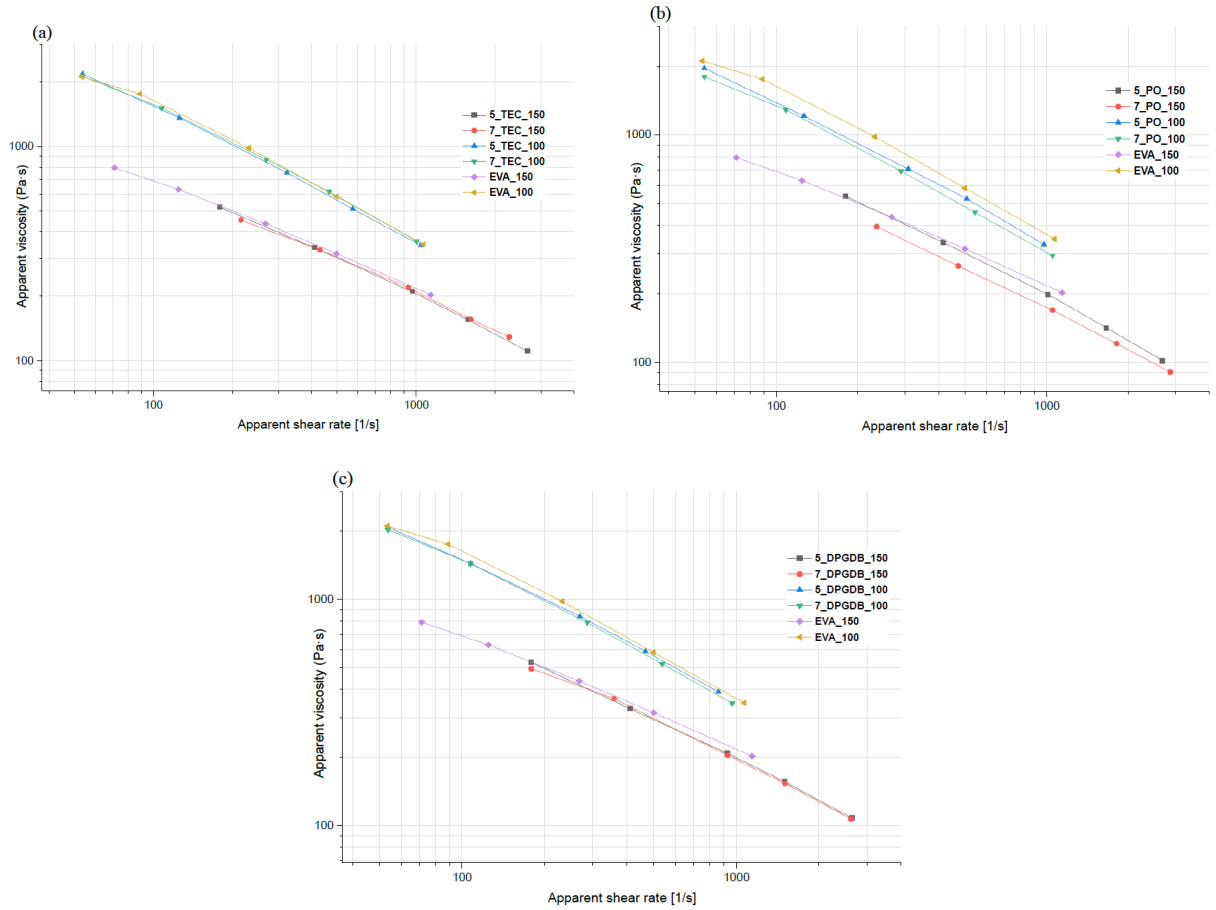


Figure 8: Apparent shear rate vs. viscosity of blends of plasticized EVA with (**a**) TEC (**b**) PO (**c**) DPGDB at 150 and 100°C.

plasticized EVA. Figure **8** presents the apparent shear rate versus apparent shear viscosity data for the plasticized blends compared with the pure EVA. The apparent shear rate and shear stress values were obtained from the instrument software; the final viscosity values were subsequently calculated from Equation (1)-(3).

It should be noted that the curves in the apparent viscosity data were plotted by connecting the experimental data points with lines for visualization. Different shear-rate ranges were obtained for each composition, in which lower temperature measurements predominantly fell within the low shear-rate regions, and those at higher temperatures fell within the high shear-rate region. The apparent viscosity was higher at the low shear rate due to higher entanglement of polymer chains at low shear rates, which restricts the flow. An important observation is that all compositions exhibited a similar viscosity range at their respective measurement temperatures, regardless of plasticizer content. In general, the plasticizers should affect the rheological behavior of the polymer, at least to some extent, as observed in the MFR measurements. In the rheological measurements, observable variations were seen only with 7_PO_150 (which was isolated from the bundle of curves) and between the measured temperatures at 100 and 150°C. However, due to the shear-thinning nature of the polymer and in order to obtain the true viscosity, the above-given apparent shear rate and viscosity data were subjected to Bagley and Weissenberg-Rabinowitsch corrections, which caused the data to shift towards the lower-right side [17].

Melt fracture is defined as waviness and uneven diameter of the extrudate, which occurs due to high shear stress on the plastic melt [13]. As mentioned by Stan *et al*. [19], certain EVA compositions exhibit melt fracture at high shear rates; nonetheless, no such phenomenon was observed for the tested composition, indicating the proper sticking of material to die walls and no slippage. At high stress, pressure-dependent slip makes the Bagley plot non-linear; in the current work, a linear approach ($R^2 > 0.99$) was used because all data points, including those at higher shear stress points, fell on a straight line, which further extends to $L/D = 0$ (ΔP_b). Figure **9** shows an example of such a plot for the pure EVA at 100 and 150°C for illustrative purposes. The resulting volumetric flow through the die, from which apparent shear rate is derived using Equation (3), is controlled by the extruder screw speed. The screw speeds used in the current work were set to 1, 2, 5, 10 and 20 RPM. However, beyond 20 RPM, the

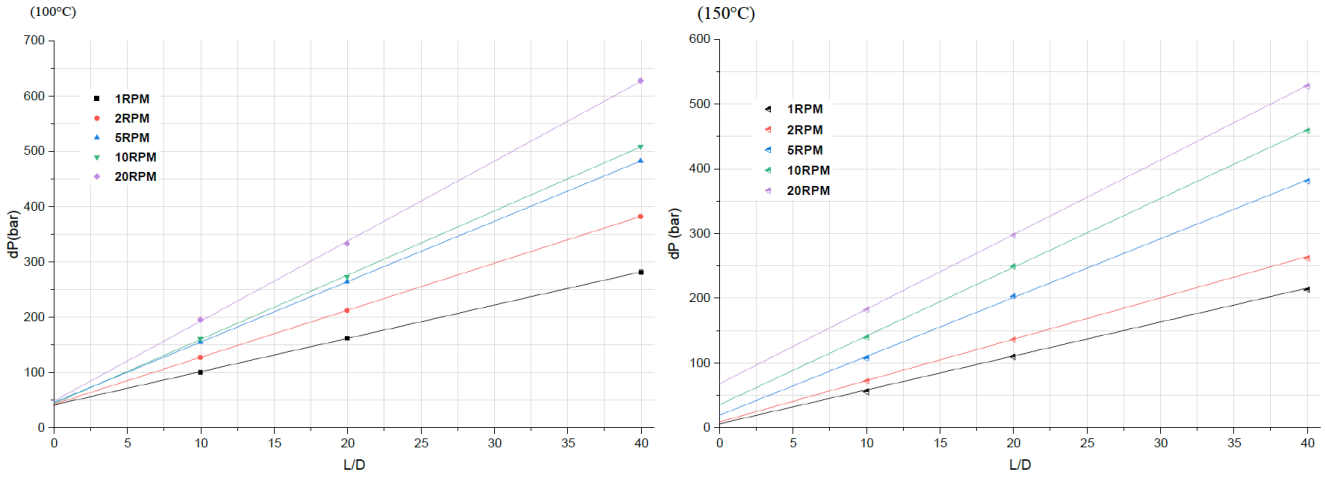


Figure 9: Bagley plot at different screw speed for Pure EVA at 100°C and 150°C.

die pressure exceeded 700 bar for the compositions measured using the 40D die at 100°C. Therefore, all measurements are limited to a maximum screw speed of 20 RPM.

It is evident from the Bagley plots that at 100°C, EVA exhibited higher $\Delta P_{measured}$, and the extrapolated pressures (ΔP_b) are closely grouped between 40 and 50 bar, compared with those at 150°C. At 150°C, ΔP_b was distributed over a range of 5 and 70 bar, suggesting the influence of temperature on the pressure gradient. A similar pattern was observed for all the plasticizer blends; however, the differences were more noticeable between the measured temperatures than between the varying plasticizer contents. After the Bagley end correction, the true wall shear stress was calculated using Equation (6).

The Weissenberg-Rabinowitsch correction, which uses the logarithmic relationship between apparent shear rate ($\dot{\gamma}_a$) and true wall shear stress (τ_w), is applied to calculate the true wall shear rate. Figure **10**-Figure **12** depicts the corrected viscosity values for the *L/D* = 40 capillary die for the TEC, PO and DPGDB blends, respectively. The markers represent the experimental data for all compositions. The solid lines for the plasticized blends measured at 100 °C and for pure EVA measured at 100 °C and 150 °C represent regression curves obtained using the CY model by Equation (10). For the plasticized blends measured at 150 °C, the experimental data points are connected by line segments, as the CY model could not be successfully fitted to these data. The experimented region covered the shear rate range of ~70-5000 s^{-1}, being within the shear-thinning region for all the blends except plasticized blends measured at 150°C. The sharp decrease in the viscosity indicates pseudoplastic behavior, where disentangled polymer chains become increasingly oriented in the direction of the flow.

All the compositions revealed similar viscosity curve shapes irrespective of the composition and temperature. In the case of TEC and DPGDB, as the plasticizer content increased (at both 100 and 150°C), the

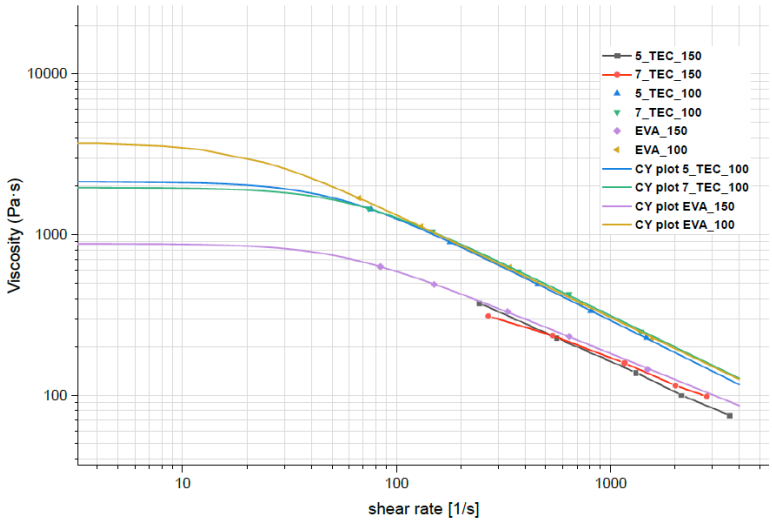


Figure 10: True shear rate vs. viscosity EVA/TEC blend.

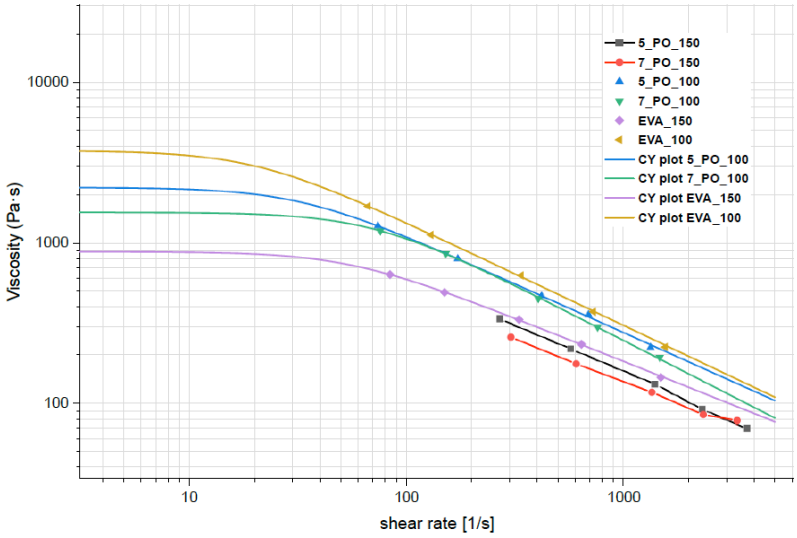


Figure 11: True shear rate vs. viscosity EVA/PO blend.

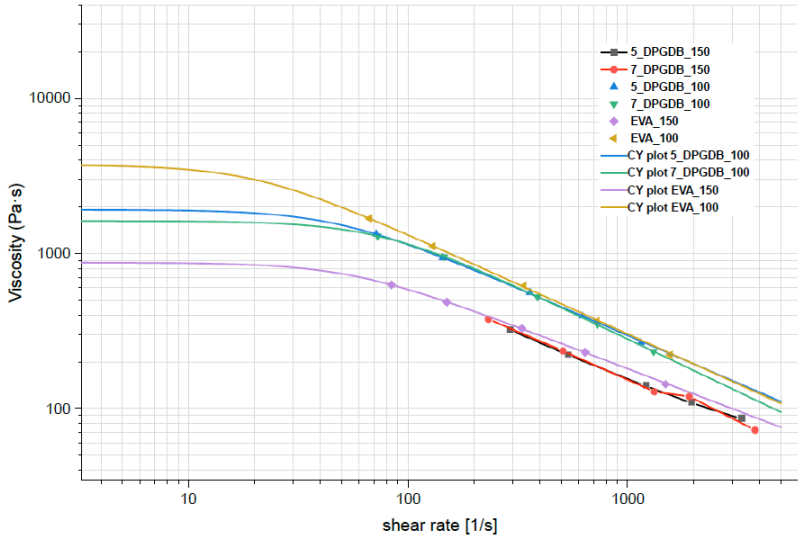


Figure 12: True shear rate vs. viscosity EVA/DPGDB blend.

viscosity values displayed comparable viscosity ranges. However, a slight variation in PO, a similar pattern to the apparent viscosity data, was observed, where the 7_PO blend showed a slight decline in the viscosity at both temperatures. See Figure **11**. The major difference seen among all the compositions, including non-plasticized EVA, is that the influence of temperature was more pronounced than the impact of plasticizer type and content in the given shear rate range. According to Dazhu *et al*. [6] and Stan *et al*. [19], temperature sensitivity of shear viscosity can be associated with the free volume concept, where higher thermal motion of polymer chains enhances the free volumes and mobility between the polymer chains. Conversely, it can be ascribed to the fact that at higher shear rates, the influence of plasticizer type and content has negligible influence on the melt viscosity, and temperature becomes the dominant factor. This is also supported by the MFR results, which represent low shear-rate measurements, where significant variation among the blends with varying plasticizer content was observed. However, the MFR results and capillary rheology measurements could not be correlated due to the differences in measurement temperatures.

The shear rate is directly proportional to the volumetric flow rate (Equation (3)). However, even at the lowest extruder screw speed, the minimum achievable shear rate for the plasticized blends measured at 150°C remained within the shear-thinning region. For neat EVA, the lowest measured shear rates were approximately 85 s^{-1} at 150°C and 67 s^{-1} at 100°C. For all the plasticizer blends measured at 100°C, the lowest measurable shear rate was approximately 74 s^{-1}, whereas for the plasticized blends measured at 150°C, it ranged between 250 and 300 s^{-1}.

The shear-thinning effect started at low shear rates below 100 s^{-1}. For both 5_DPGDB_100 and 7_DPGDB _100, shear thinning was observed from circa 65 s^{-1},

whereas for the 5_TEC_100 and 7_TEC_100, it started at approximately 30 s^{-1}. In contrast, the PO blends exhibited the earliest onset of shear thinning, with 5_PO_100 and 7_PO_100 starting at around 20 s^{-1} and 30 s^{-1}, respectively. The CY model parameters are summarized in Table **3**. The fitted parameters are reported for plasticized blends at 100°C and pure EVA at 100 and 150°C. Within each table cell, the values are presented in the order of η_o, λ and *n* separated by a semicolon. It is important to note that the viscosity values estimated using the CY model should be considered with caution, as they are not experimental numbers. Moreover, the use of a smaller die radius (0.5 mm) resulted in higher wall shear rates for the plasticized blends at 150°C due to the inverse cubic relationship between die radius and the shear rate (from Equation (3)). Consequently, the dataset was concentrated mostly in the higher shear-rate region, providing insufficient low-shear-rate data for the accurate prediction of zero-shear viscosity. According to the CY model regression, the flow behavior index *n* for the blends measured at 100 °C ranged from 0.30 to 0.37. The lowest value was observed for the 7_PO blend, whereas pure EVA exhibited *n* values of 0.31 and 0.46 at 100 °C and 150 °C, respectively.

Table 3: CY-Model Parameters of Plasticized Blends of 5 and 7 phr at 100°C and Pure EVA at 100°C and 150°C

Composition	5 phr	7 phr
EVA/TEC_100	2397 ; 0.02 ; 0.32	2263 ; 0.02 ; 0.33
EVA/PO_100	2161 ; 0.02 ; 0.37	1890 ; 0.01 ; 0.30
EVA/DPGDB_100	2056 ; 0.02 ; 0.36	1938 ; 0.01 ; 0.31
EVA_100	2585 ; 0.02 ; 0.319	
EVA_150	871 ; 0.018 ; 0.46	

The CY model regression showed a good fit to the experimental data for the compositions with R^2 values greater than 0.99. However, regression analysis using the CY model could not be performed for the plasticized blends measured at 150 °C. This was primarily due to the lack of sufficient viscosity data in the low-shear-rate region (<100 s^{-1}), which is crucial for estimating the zero-shear viscosity. This limitation should be considered a consequence of insufficient experimental data at low shear rates rather than the intrinsic material response. The predicted CY model η_o values at 100°C indicate that increasing the plasticizer content from 5 to 7 phr lowered the viscosity in all plasticized blends. On the other hand, for the pure EVA, η_o is at 2585 Pa·s for measurements at 100°C and 871 Pa·s for measurements at 150°C. The EVA/TEC blend showed a predicted zero shear viscosity reduction from 2397 and 2263 Pa·s, while the EVA/PO and EVA/DPGDB blends showed reductions from 2161 to 1890 Pa·s and 2056 to 1938 Pa·s, respectively. Among the plasticizers, the PO blend showed the largest reduction, indicating better compatibility and plasticization efficiency in the low shear rate region, which is also strongly supported by MFR results, which showed the highest MFR values among all the blends. From the measurements made at 100°C for the plasticized blends. The viscosity at considered shear rate ranges in the FGF process could be considered too high, where the screw low L/D would struggle at higher print speed and disrupt the constant flow.

CONCLUSIONS AND SUMMARY

In this study, the behavior of EVA plasticized with TEC, PO and DPGDB at 1, 3, 5 and 7 phr was investigated using thermal and rheological characterizations. The main objective was to study the rheology over a wide shear-rate range for applications requiring reduced melt viscosity, particularly for FGF 3D printing with low *L/D* ratio screws.

The MFI results showed that increasing plasticizer content generally increased the MFI. Among all the compositions, the most linear increase and the highest MFI were observed in the PO/EVA blend. However, the 7 phr DPGDB blend showed a sudden drop in MFI, while the 7 phr TEC exhibited plasticizer bleed-out during compounding, suggesting a saturation point at higher plasticizer loadings.

DSC analysis showed a consistent trend of decreasing melting temperature with a slight increase in the degree of crystallinity for the plasticized blends compared with pure EVA. However, no correlation between plasticizer content and crystallinity was observed.

The capillary rheological data for all 5 and 7 phr compositions were subjected to Bagley and Weissenberg-Rabinowitsch corrections to determine the true viscosity. All the blends exhibited shear thinning behavior. The CY model showed an excellent fit for the plasticizer blends measured at 100°C and for pure EVA blends. Increasing the plasticizer content from 5 to 7 phr showed a slight variation in the predicted curve and a reduction in η_o for all blends. All compositions exhibited strong shear-thinning at lower shear-rate conditions due to the earlier polymer chain-enforced alignment, followed by a rapid decrease in viscosity, while the highest reduction was observed in PO blends, indicating greater plasticization efficiency under low shear rates. However, regression for the blends measured at 150°C could not be accurately determined because the experimental measurements did not adequately cover the low shear-rate region.

From the experimental rheological plots, no visible viscosity variation between 5 and 7 phr was observed for any plasticizer system in the shear thinning region at higher shear rates. The main difference observed was between measurements at 100°C and 150°C, where the lower processing temperature consistently showed higher viscosity. This suggests that, within the studied shear-rate range, the rheological response is primarily controlled by temperature. Based on the measurements at 100 °C, the viscosities of the plasticized blends within the shear rate range relevant for the FGF process could be considered too high, potentially making it difficult for the low-L/D-ratio screws to operate at higher printing speeds and maintain a constant material flow. The online capillary rheometer is well suited for shear viscosity measurements; however, the present study also demonstrates that appropriate selection of the capillary die diameter for online capillary rheology could be essential to access the low shear-rate regions for the higher temperature measurements. Further studies will focus on exploring alternative plasticizers such as dioctylphthalates and selecting suitable plasticizers based on their solubility parameters and evaluating their influence on the foaming behavior of EVA in conventional and FGF 3D printing processes.

ACKNOWLEDGEMENTS

The authors gratefully acknowledge the financial support provided by the German Federal Ministry for Economic Affairs and Climate Protection (Bundesministerium für Wirtschaft und Klimaschutz, BMWK) through the Central Innovation Programme for SMEs (ZIM), under project reference number KK5225904KL4. The authors sincerely thank the Institut für Kunststofftechnik Westpfalz (IKW), Hochschule Kaiserslautern, for providing the laboratory facilities, equipment, and technical resources necessary for this research. The authors would like to thank Jürgen Dully (technical employee) for his support and guidance during the measurements.

AUTHORS CONTRIBUTION

Praneeth D. Bangaru: Conceptualization, investigation, data analysis, and writing. Terezie Pospíšilíková: Investigation, data analysis, and experimental work. Tharcisse Renzahoduke: Experimental work. Jens Schuster: Supervision and project administration. All authors reviewed and agreed to the published version of the manuscript.

CONFLICT OF INTEREST

The author declared no conflicts of interest.

REFERENCES

[1] Arsac A, Carrot C, Guillet J. Rheological characterization of ethylene vinyl acetate copolymers. J. Appl. Polym. Sci. 1999; 74: 2625-30. https://doi.org/10.1002/(SICI)1097-4628(19991209)74:11<2625::AID-APP9>3.0.CO;2-G

[2] Henderson AM. Ethylene-vinyl acetate (EVA) copolymers: a general review. IEEE Electr. Insul. Mag. 1993; 9: 30-8. https://doi.org/10.1109/57.249923

[3] Zhang Y, Wang Z, Li C, Chen Z, Fang P. Correlation Study between the Rheological Property and the Free Volume for Ethylene Vinyl Acetate Copolymer under Melt Extrusion. 2014. https://doi.org/10.56646/jjapcp.2.0_011201

[4] Matheus VG Zimmermann, Marcos Aurélio Colombo, Diego Pizza, and Ademir J Zattera. Influence on the cross-linking and plasticization degree of poly(ethylene-co-vinyl acetate) and evaluation of expansion capacity to the production of foams with supercritical CO2.

[5] Standring T, Blackburn S, Wilson P. Investigation into Paraffin Wax and Ethylene Vinyl Acetate Blends for Use as a Carrier Vehicle in Ceramic Injection Molding. Polymer-Plastics Technology and Engineering. 2016; 55: 802-17. https://doi.org/10.1080/03602559.2015.1132434

[6] Dazhu Chen, Weian Zhang, and Pingsheng He. Capillary Extrusion Rheology and Thermal Stability of EVA/Organomontmorillonite Nanocomposites. 2004: 271-80. https://doi.org/10.1177/096739110501300307

[7] Jang HK, Oh Y, Hwang WR. Experimental in-situ viscosity measurement of polymer melts in a film extrusion die. Chemical Engineering Science. 2025; 305: 121139. https://doi.org/10.1016/j.ces.2024.121139

[8] Wypych G. Handbook of plasticizers. 4th ed. Toronto: ChemTec Publishing; 2023. https://doi.org/10.1016/B978-1-77467-022-4.50005-1

[9] Chen Z, Fang P, Wang H, Zhang S, Wang S. Property of ethylene vinyl acetate copolymer in melting processing. J of Applied Polymer Sci. 2006; 101: 2022-6. https://doi.org/10.1002/app.23767

[10] Das A, Gilmer EL, Biria S, Bortner MJ. Importance of Polymer Rheology on Material Extrusion Additive Manufacturing: Correlating Process Physics to Print Properties. ACS Appl. Polym. Mater. 2021; 3: 1218-49. https://doi.org/10.1021/acsapm.0c01228

[11] Curmi A, Rochman A. From Theory to Practice: Development and Calibration of Micro Pellet Extruder for Additive Manufacturing. KEM. 2022; 926: 34-45. https://doi.org/10.4028/p-b22a9a

[12] Curmi A, Rochman A. Miniaturized fused granulate fabrication of polyether ether ketone (PEEK). Prog Addit Manuf. 2024; 9: 1265-75. https://doi.org/10.1007/s40964-023-00518-4

[13] Henrichs NN, Sehrt JT, Brinkmann T, Bürgel LPM, Berger DM. Influence of Flowability on the Processability of Thermoplastics in Additive Manufacturing: Comparison of Fused Layer Modeling (FLM) and Fused Granulate Fabrication (FGF). J of Applied Polymer Sci 2026. doi: 10.1002/app.71048. https://doi.org/10.1002/app.71048

[14] Volotskoy AN, Yurkin YV, Avdonin VV. Influence Study of Plasticizer Compatibility on Strength Properties of Ethylene-Vinyl Acetate. MSF. 2018; 935: 79-83. https://doi.org/10.4028/www.scientific.net/MSF.935.79

[15] Lu H, Liu M, Ruan C, Su L, Yan H, Wang H. Practicality of bioderived coconut oil as a plasticizer for ethylene propylene diene monomer. Industrial Crops and Products. 2025; 224: 120342. https://doi.org/10.1016/j.indcrop.2024.120342

[16] Luger H-J, Miethlinger J. Development of an online rheometer for simultaneous measurement of shear and extensional viscosity during the polymer extrusion process.

Polymer Testing. 2019; 77: 105914. https://doi.org/10.1016/j.polymertesting.2019.105914

[17] Wilczyński KJ, Buziak K, Lewandowski A, Wilczyński K. Rheology for Wood Plastic Composite Extrusion-Part 1: Laboratory vs. On-Line Rheometry. Polymers (Basel) 2025. https://doi.org/10.3390/polym17202782

[18] McAfee M, McNally G. Real-time measurement of melt viscosity in single-screw extrusion. Transactions of the Institute of Measurement and Control. 2006; 28: 481-97. https://doi.org/10.1177/0142331206069478

[19] Stan F, Stanciu NV, Fetecau C. Melt rheological properties of ethylene-vinyl acetate/multi-walled carbon nanotube composites. Composites Part B: Engineering. 2017; 110: 20-31. https://doi.org/10.1016/j.compositesb.2016.10.071

[20] Ferreira IP, Da Sirqueira AS, Santos TAd, Naccache MF, Soares BG. Rheological studies of SBS/EVA blends modified with bio-based cashew nut shell liquid. Journal of Elastomers & Plastics. 2021; 53: 825-40. https://doi.org/10.1177/0095244321990407

[21] Rides M, Kelly AL, Allen CR. An investigation of high rate capillary extrusion rheometry of thermoplastics. Polymer Testing. 2011; 30: 916-24. https://doi.org/10.1016/j.polymertesting.2011.08.011

[22] Agroui K, Collins G, Farenc J. Measurement of glass transition temperature of crosslinked EVA encapsulant by thermal analysis for photovoltaic application. Renewable Energy. 2012; 43: 218-23. https://doi.org/10.1016/j.renene.2011.11.015

https://doi.org/10.31875/2410-4701.2026.13.09

© 2026 Bangaru *et al.*
This is an open-access article licensed under the terms of the Creative Commons Attribution License (http://creativecommons.org/licenses/by/4.0/), which permits unrestricted use, distribution, and reproduction in any medium, provided the work is properly cited.